Studies of Vector Boson Scattering And Triboson Production with Delphes Parametrized Fast Simulation of SnowMass 2013

C. Degrande, O. Eboli, J. L. Holzbauer, S.-C. Hsu, A. Kotwal, S. Li, M. Marx, O. Mattelaer, J. Metcalfe, M-A. Pleier, C. Pollard, M. Rominsky, D. Wackeroth

July 24, 2013

1 Introduction

In the Standard Model, the only allowed quartic couplings are $WWWW, WWZZ, WWZ\gamma$ and $WW\gamma\gamma$ and they are completely specified. Measuring these couplings will provide stringent tests to the Standard model and help searches for physics beyond the standard model. The standard way to search for these couplings is to measure triboson production. WWW production probes $WWWW$, while WWZ and $WW\gamma$ probe $WWZZ, WWZ\gamma$ and $WW\gamma\gamma$, respectively [?]. This section focusses first on WWW, WWZ, WZZ and ZZZ with a quick scan of the energies and cross sections, and then a case study from WWW is highlighted with the promising operators.

This analysis is carried out using effective Lagrangian theory [?]. The details are explained in a separate document. We tested both dimension 6 operators (list operators here) and dimension 8 operators. Since dim6 operators are sensitive to both triple and quartic gauge couplings, we found that these operators didn't show much sensitivity. However, dim8 is only sensitive to quartic gauge couplings and are therefore where we put our energy.

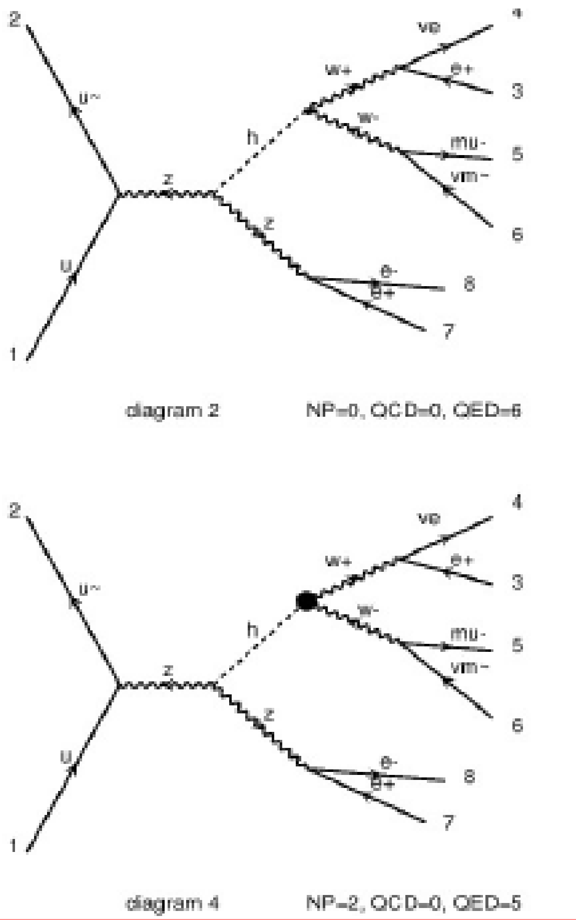

Figure 1: Feynman diagrams from MadGraph [?] for the $WWZZ$ process.

Figure 1 shows example diagrams for the $WWZZ$ process. This Snowmass exercise was performed using MadGraph [?] for event generation, Pythia for showering, a special version of Delphes [?] for the detector simulation and specially designed pile up files [?].

1.1 Effective theory with dimension 6 operators

The dimension 6 operators that we looked at were C_W, C_{WWW} and C_b. Table 1.1 shows the cross section scan performed

Operator	C_W	Coupling value	5
Process	machine	energy	XSection
WWZ	LHC	14 TeV	number
WWW	LHC	14 TeV	number
WZZ	LHC	14 TeV	number
Operator	C_{WWW}	Coupling value	5
Operator	C_b	Coupling value	5

Table 1: Dimension 6 operators

1.2 Effective theory with dimension 8 operators

Dimension 8 operators are only sensitive to quartic gauge couplings and offer a good way to explore anomalous couplings. The dimension 8 operators sensitive to WWW, WWZ, WZZ and ZZZ are listed in Table 2 .

Table 2: default

	$WWWW$	$WWZZ$	$ZZZZ$
$\mathcal{L}_{S,0}$, $\mathcal{L}_{S,1}$	X	X	X
$\mathcal{L}_{M,0}$, $\mathcal{L}_{M,1}$,$\mathcal{L}_{M,6}$, $\mathcal{L}_{M,7}$	X	X	X
$\mathcal{L}_{M,2}$, $\mathcal{L}_{M,3}$,$\mathcal{L}_{M,4}$, $\mathcal{L}_{M,5}$	O	X	X
$\mathcal{L}_{T,0}$, $\mathcal{L}_{T,1}$,$\mathcal{L}_{T,3}$	X	X	X
$\mathcal{L}_{T,5}$, $\mathcal{L}_{T,6}$,$\mathcal{L}_{T,7}$	O	X	X
$\mathcal{L}_{T,8}$, $\mathcal{L}_{T,9}$	O	O	X

2 VBS $WZ \to \ell\nu\ell\ell$

We parameterize new physics in this channel using the dimension-8 operator

$$\mathcal{L}_{T,1} = \frac{f_{T1}}{\Lambda^4} \mathrm{Tr}[\hat{W}_{\alpha\nu}\hat{W}^{\mu\beta}] \times \mathrm{Tr}[\hat{W}_{\mu\beta}\hat{W}^{\alpha\nu}] \tag{1}$$

and dimension-6 operator

$$\mathcal{L}_{\phi d} = \frac{c_{\phi d}}{\Lambda^2} \partial_\mu(\phi^\dagger\phi)\partial^\mu(\phi^\dagger\phi) \tag{2}$$

The fully leptonic $WZjj \to \ell\nu\ell\ell jj$ channel has a larger cross section than $ZZjj \to \ell\ell\ell\ell jj$ and can still be reconstructed by solving for the neutrino p_z using the W boson mass constraint.

In order to use the W mass constraint, the lepton from W decay must first be identified. If two lepton flavors occur in an event, the unpaired lepton is assumed to come from the W boson. If all three leptons have the same flavor, the invariant masses of all combinations of opposite-sign pairs are calculated, and the pair whose mass is closest to the Z mass is called the Z pair; the unpaired lepton is then used in the neutrino p_z determination.

In the event that there are multiple neutrino p_z solutions to the W mass constraint equation, the solution with the smallest magnitude is chosen. If no real p_z solution exists, the x and y components of $E_{\mathrm{T}}^{\mathrm{miss}}$ are varied minimally to give a unique solution.

Figure 2 and 4 shows the reconstructed 4-lepton invariant mass distribution for this channel.

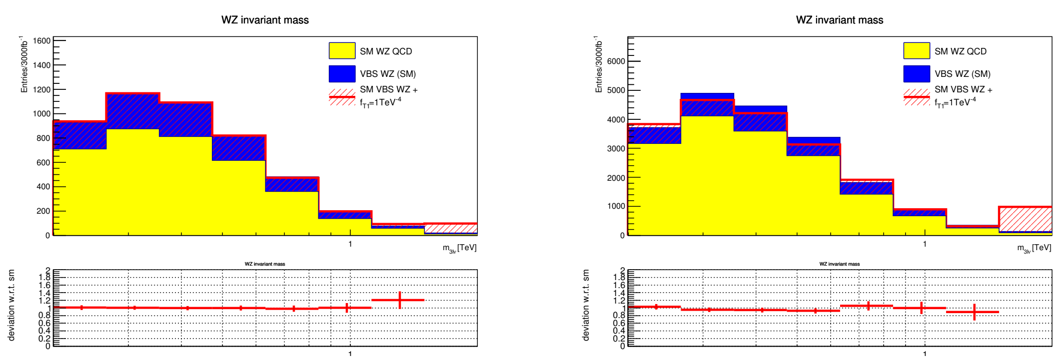

Figure 2: In the $pp \to WZ + 2j \to \ell\nu\ell\ell + 2j$ channel, the reconstructed WZ mass spectrum comparisons between Standard Model and dimension-8 operator coefficient $f_{T1}/\Lambda^4 = 1TeV^{-4}$ are shown using the charged leptons and the neutrino solution after requiring $m_{jj} > 1$ TeV at $\sqrt{s} = 14$ TeV (left) and 33 TeV (right). The overflow bin is included in the plots.

2.1 Monte Carlo Predictions

We include only the SM WZ production as background, as ATLAS analyses of current data [1] have shown that mis-identification backgrounds are small in this channel. Non-VBS WZ production in association with initial-state radiation of two jets was

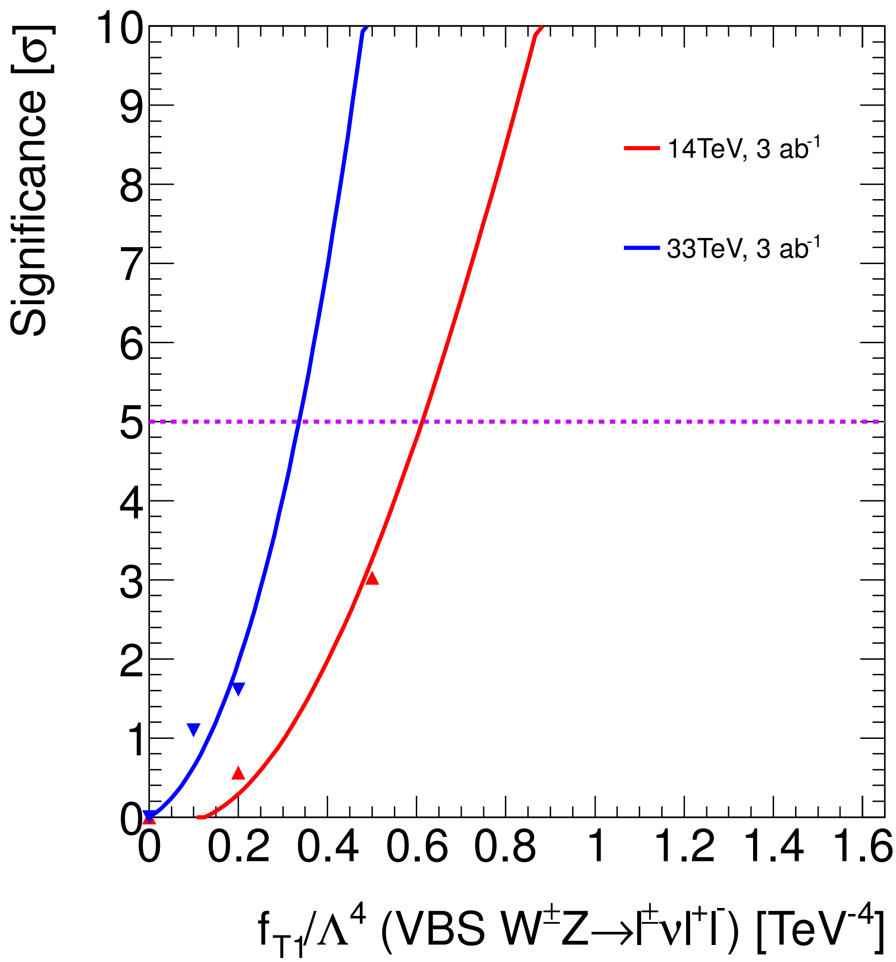

Figure 3: $pp \to WZ + 2j \to \ell\nu\ell\ell + 2j$ signal significance as a function of f_{T1}/Λ^4 calculated from reconstructed WZ mass spectra at $\sqrt{s} = 14$ TeV and 33 TeV.

simulated using MadGraph [2]. MadGraph 1.5.10 was used to generate SM and non-SM VBS WZ production. Each W boson was required to decay to an electron and neutrino or a muon and neutrino, and each Z boson was required to decay to an electron or muon pair.

2.2 Event Selection

Events are considered VBS WZ candidates provided they meet the following criteria:

- Exactly three selected leptons (each with $p_T > 25$ GeV) which can be separated into an opposite sign, same flavor pair and an additional single lepton
- At least one selected lepton must fire the trigger.
- At least two selected jets with $p_T > 50$ GeV.
- $m_{jj} > 1$ TeV, where m_{jj} is the invariant mass of the two highest-p_T selected jets

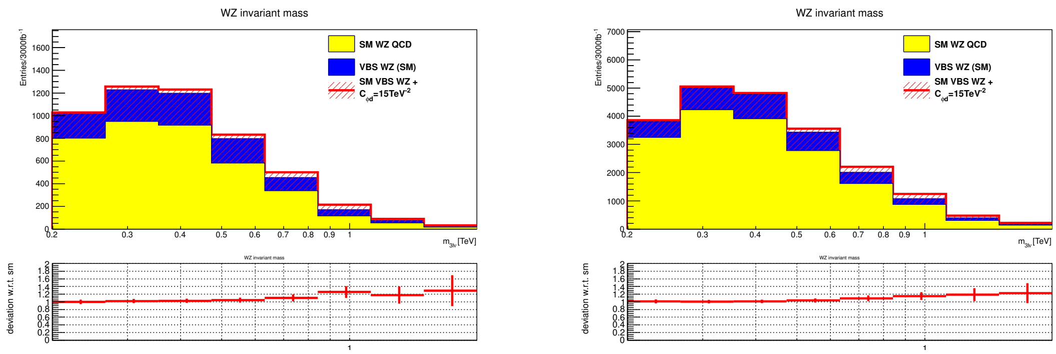

Figure 4: In the $pp \to WZ + 2j \to \ell\nu\ell\ell + 2j$ channel, the reconstructed WZ mass spectrum comparison between Standard Model and dimension-6 operator coefficient $c_{\phi d}/\Lambda^2 = 15TeV^{-2}$ using the charged leptons and the neutrino solution after requiring $m_{jj} > 1$ TeV at $\sqrt{s} = 14$ TeV (left) and 33 TeV (right). The overflow bin is included in the plot on the left.

2.3 Statistical Analysis

The statistical analysis is identical to that employed in Sec. 3.3. Figure 3 and 5 shows the signal significance as a function of f_{T1}/Λ^4 and $c_{\phi d}/\Lambda^2$. In Table 3 the 5σ discovery potential is illustrated, showing the improvement possible with the increased luminosity. As in the $ZZ \to 4\ell$ channel, the reconstructed $3\ell\nu$ mass is the process $\sqrt{\hat{s}}$, and the study of its distribution directly probes the energy-dependence of the new physics.

Parameter	dimension	14 TeV		33 TeV	
		5σ	95% CL	5σ	95% CL
$c_{\phi d}/\Lambda^2$	6	15.0 TeV^{-2}	8.7 TeV^{-2}	11.2 TeV^{-2}	6.6 TeV^{-2}
f_{T1}/Λ^4	8	0.6 TeV^{-4}	0.4 TeV^{-4}	0.3 TeV^{-4}	0.2 TeV^{-4}

Table 3: In $pp \to WZ + 2j \to \ell\nu\ell\ell + 2j$ processes, 5σ-significance discovery values and 95% CL limits for coefficients of higher-dimension operators with 3000 fb^{-1} of integrated luminosity.

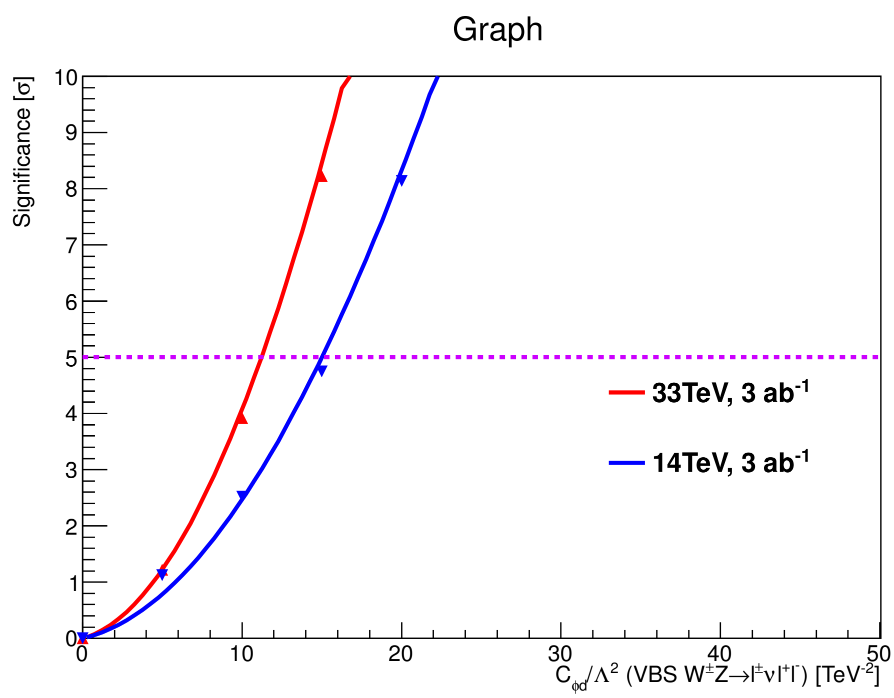

Figure 5: $pp \to WZ + 2j \to \ell\nu\ell\ell + 2j$ signal significance as a function of $c_{\phi d}/\Lambda^2$ calculated from reconstructed WZ mass spectra at $\sqrt{s} = 14$ TeV and 33 TeV.

3 VBS $ZZ \to \ell\ell\ell\ell$

In this channel, the following new analysis has been performed since the European Strategy Submission [3], based on the dimension-6 operator

$$\mathcal{L}_{\phi W} = \frac{c_{\phi W}}{\Lambda^2} \mathrm{Tr}(W^{\mu\nu} W_{\mu\nu}) \phi^\dagger \phi \tag{3}$$

The fully-leptonic $ZZjj \to \ell\ell\ell\ell jj$ channel has a small cross section but provides a clean, fully reconstructible ZZ final state. A forward jet-jet mass requirement of 1 TeV reduces the contribution from jets accompanying non-VBS diboson production.

3.1 Monte Carlo Predictions

We include only the SM ZZ production as background, as ATLAS analyses of current data [4] have shown that mis-identification backgrounds are small in this clean channel. SM and non-SM ZZ production MadGraph 1.5.10 is used in SM and non-SM ZZ production as well as the non-VBS background generation. The non-VBS background are generated with the accompany of the initial-state radiation of two jets. In both cases Z bosons were required to decay to electron or muon pairs.

3.2 Event Selection

Events are considered VBS ZZ candidates provided they meet the following criteria:

- Exactly four selected leptons (each with $p_T > 25$ GeV) which can be separated into two opposite sign, same flavor pairs (No Z mass window requirement)
- At least one selected lepton must fire the trigger.
- At least two selected jets, each with $p_T > 50$ GeV
- $m_{jj} > 1$ TeV, where m_{jj} is the invariant mass of the two highest-p_T selected jets

3.3 Statistical Analysis

In order to determine the expected sensitivity to BSM ZZ contribution, the background-only p_0-value expected for signal+background is calculated using the $m_{4\ell}$ spectrum.

Parameter	dimension	14 TeV		33 TeV	
		5σ	95% CL	5σ	95% CL
$c_{\phi W}/\Lambda^2$	6	16.0 TeV^{-2}	9.7 TeV^{-2}	13 TeV^{-2}	7.7 TeV^{-2}

Table 4: In $pp \to ZZ + 2j \to \ell\ell\ell\ell + 2j$ processes, 5σ-significance discovery values and 95% CL limits for coefficients of higher-dimension operators with 3000 fb^{-1} of integrated luminosity.

Figure 6 shows the reconstructed 4-lepton invariant mass distribution. Figure 7 shows signal significance as a function of $c_{\phi W}/\Lambda^2$.

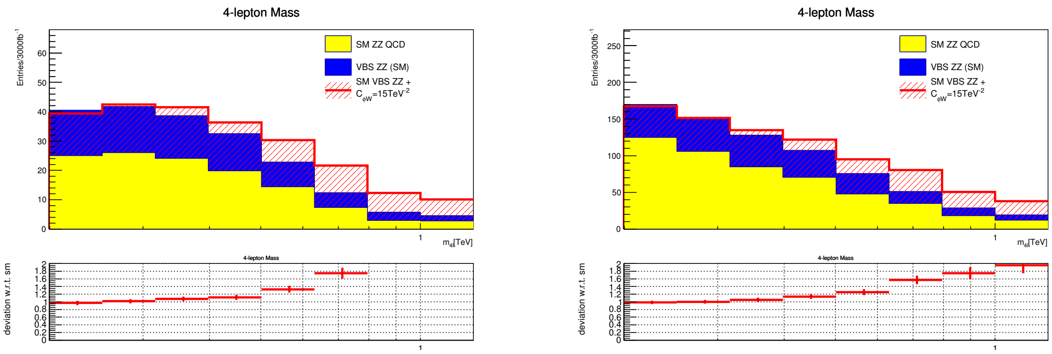

Figure 6: In the $pp \to ZZ + 2j \to \ell\ell\ell\ell + 2j$ process, the reconstructed 4-lepton mass ($m_{4\ell}$) spectrum comparisons between Standard Model and dimension-6 operator coefficient $c_{\phi W}/\Lambda^2 = 15TeV^{-4}$ are shown after requiring $m_{jj} > 1$ TeV at $\sqrt{s} = 14$ TeV (left) and 33 TeV (right). The overflow bin is included in the plots.

In Table 4 the 5σ discovery potential is illustrated, showing the improvement possible with the increased luminosity. Since the $4-$lepton mass is the process $\sqrt{\hat{s}}$, the study of its distribution directly probes the energy-dependence of the new physics.

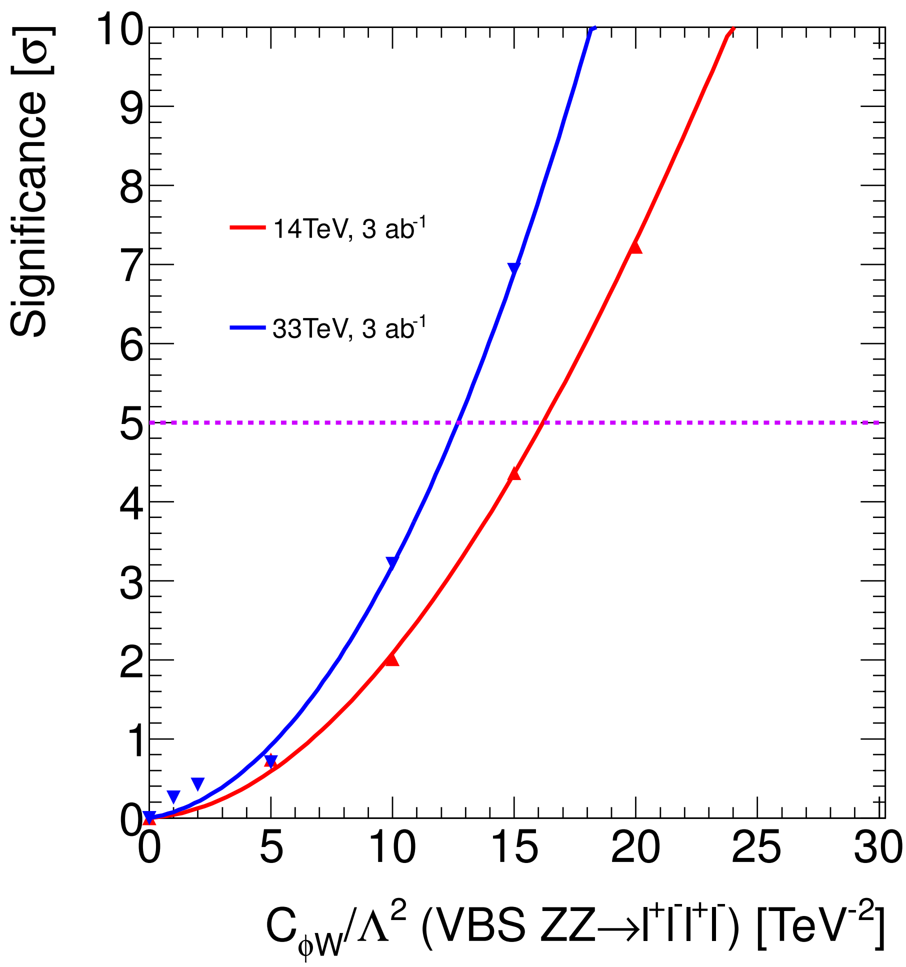

Figure 7: $pp \to ZZ + 2j \to \ell\ell\ell\ell + 2j$ signal significance as a function of $c_{\phi d}/\Lambda^4$ calculated from reconstructed ZZ mass spectra at $\sqrt{s} = 14$ TeV and 33 TeV.

4 $WWZ \to 5l$

The C_W operator was studied first. All processes studied were decayed fully leptonically. Figure 8 hows the number of events versus machine energy for each of the three processes with the SM)C_W set to 0) and the C_W operator set to a value of 5. The WZZ anomalous coupling shows a distinct difference between the SM shape and anomalous coupling, but between backgrounds and the low event rate, this is not a very promising channel. Figure 9 shows the invariant mass of five leptons for 2 different machine energies, with 50,000 events, and requiring all five leptons.

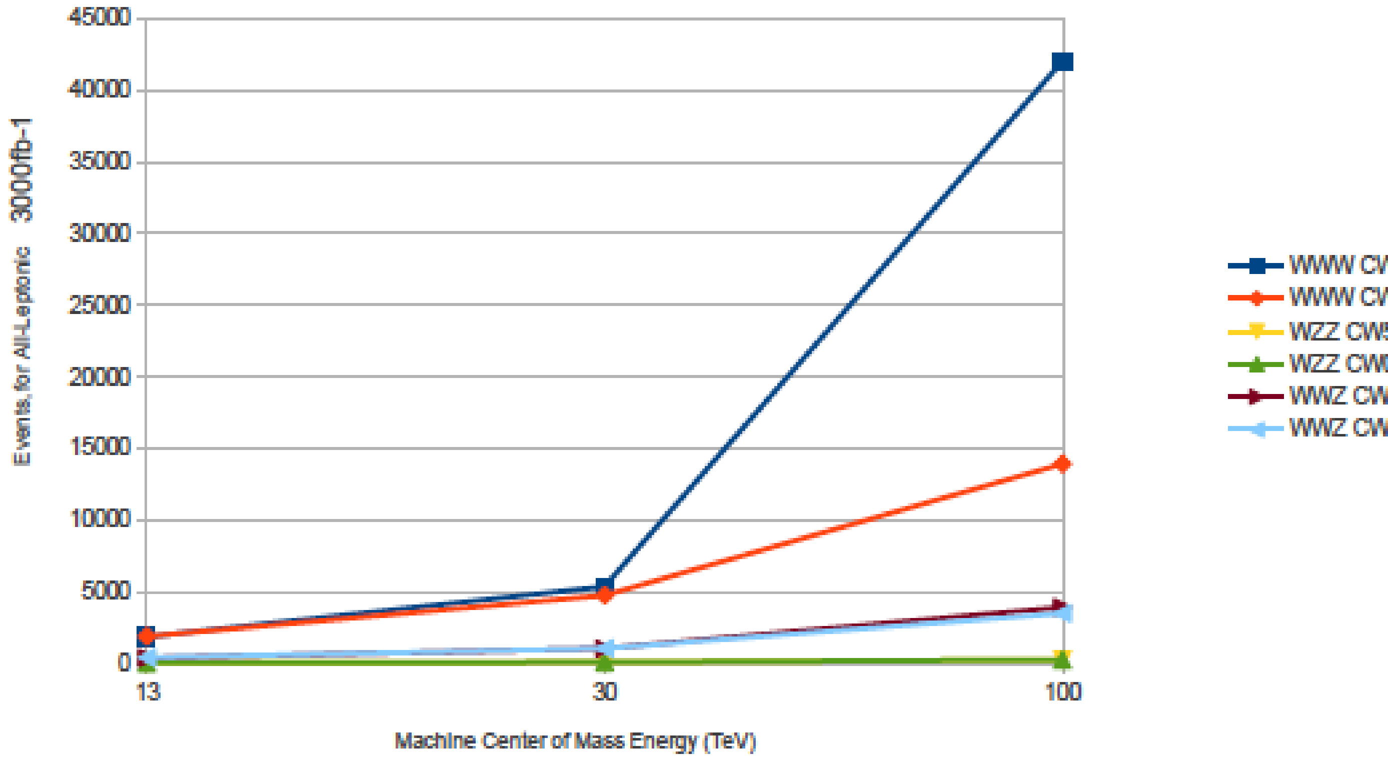

Figure 8: Number of Events for different machine energies with the C_W operator set to 5 and set to 0, which is the Standard Model case.

The WWZ processes has more background when requiring four leptons, as compared to WZZ, but the signal rate is also expected to be higher. Figure 10 shows the invariant mass for this process when requiring 4 leptons for two different machine energies.

Finally, the WWW process has the largest cross section for the anomalous coupling, but it also will have more trouble with backgrounds 11.

In addition to testing C_W, the C_{WWW} and C_b operators were probed. The C_b operator showed no sensitivity to anomalous couplings, but the C_{WWW} operator shows a larger sensitivity than C_W 12.

While some of the dimension 6 operators showed reasonable sensitivity to anomalous couplings, we decided to focus on the dimension 8 operators because they are more sensitive to the quartic couplings.

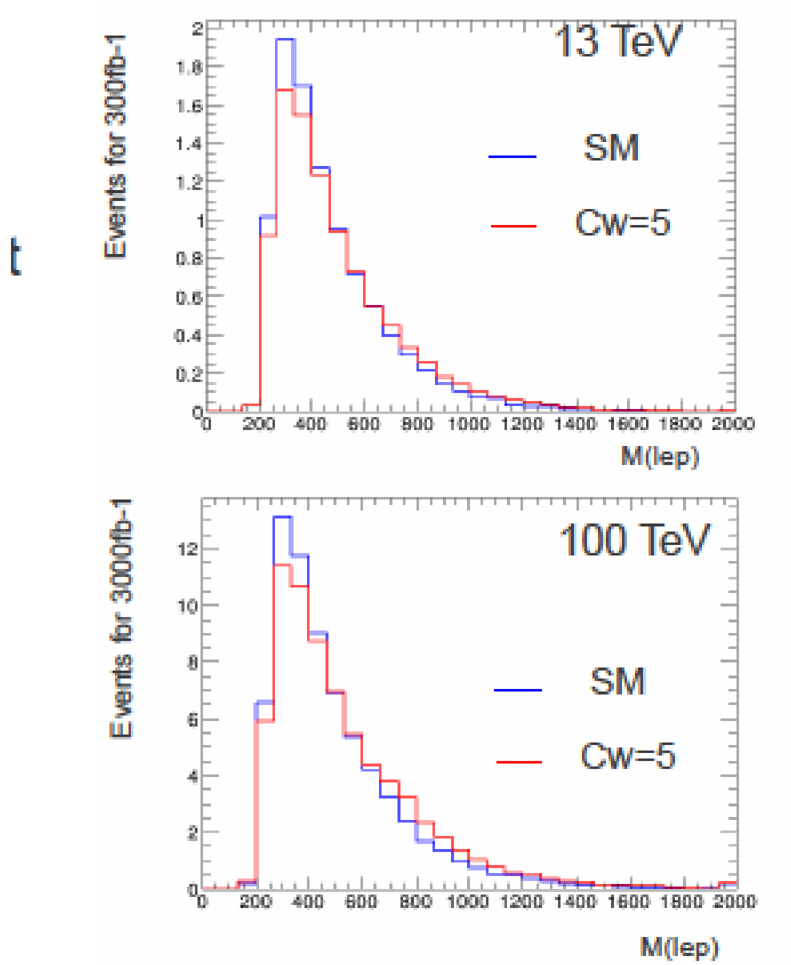

Figure 9: Invariant mass of the 5 leptons in the WZZ channel in the SM case (blue) and with C_W turned on (red).. There are 50,000 events in the sample and a cut requiring exactly 5leptons. Background is not included in this plot.

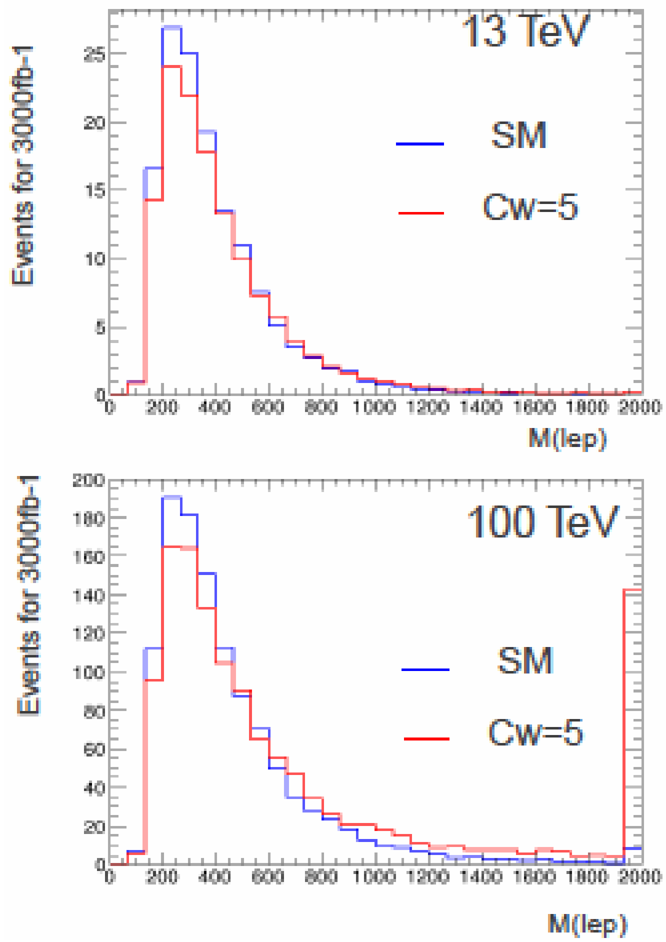

Figure 10: WWZ process with SM (blue) and C_W, 50,000 events and requiring 4 leptons.

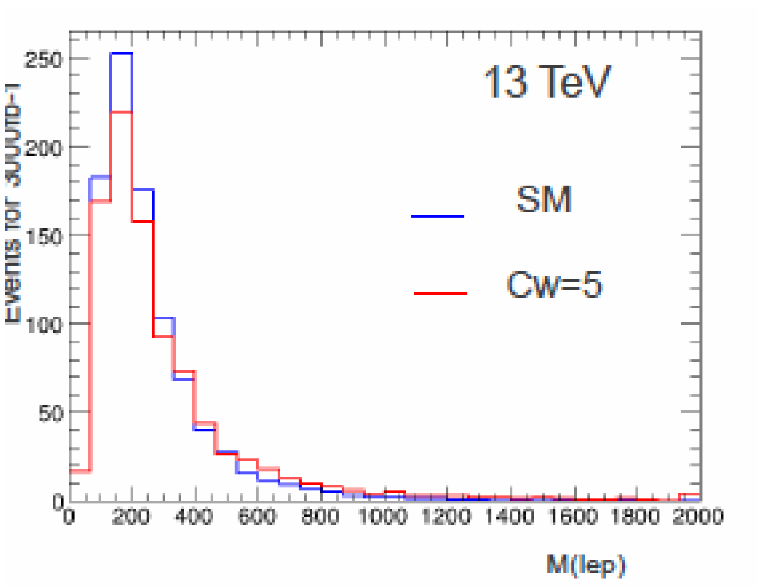

Figure 11: Invariant mass for WWW at 13 TeV with the SM (blue) and C_W (red).

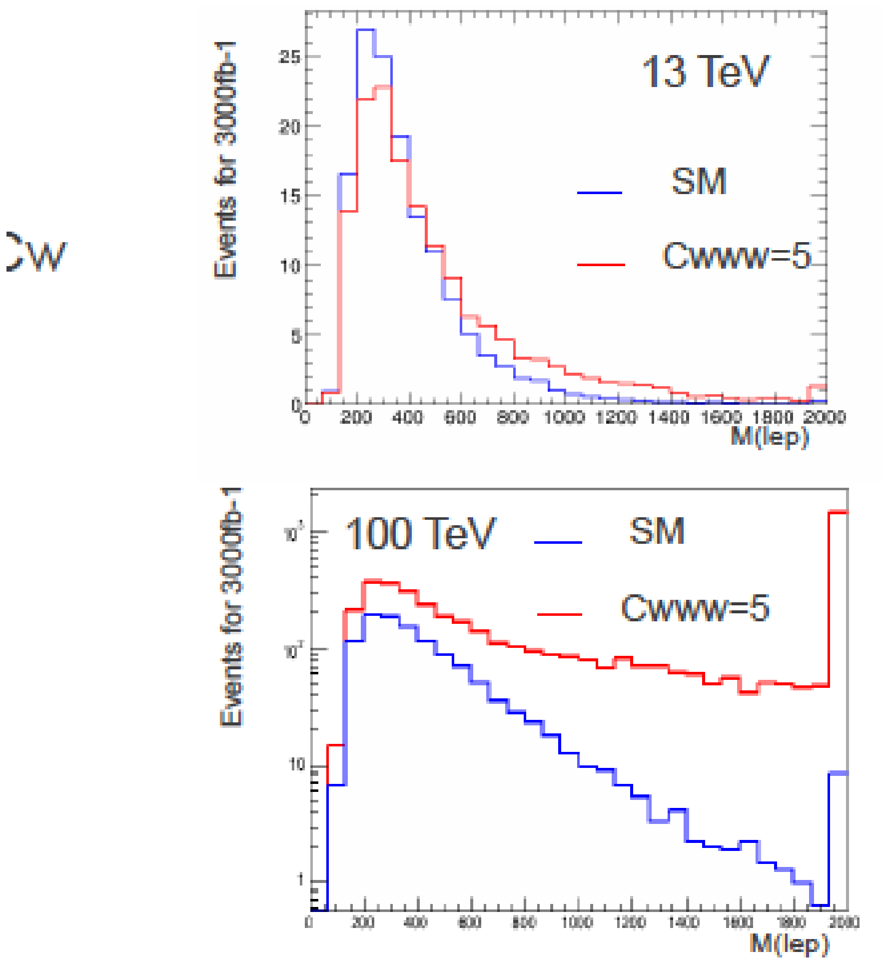

Figure 12: The WWW invariant mass with the SM (blue) and C_{WWW} operator set to 5.

5 $WWW \to 5l$

An extensive cross section scan was performed to compare the SM cross sections to anomalous coupling cross sections for various coupling values and machine energies (Table 5). From the study, the T0 operator was found to be the most sensitive to anomalous couplings, particularly in the WWW channel.

Coupling SM Cross Section (pb)	WWW 0.000568000	WWZ 0.000111800	WZZ 0.000009634	ZZZ 0.000000972
sm/sm	1.0	1.0	1.0	1.0
fs0/sm	1.0	1.0	1.0	1.0
fs1/sm	1.0	1.0	1.0	1.0
fm0/sm	1.49	1.09	1.05	1.02
fm1/sm	1.18	1.02	1.04	1.03
fm2/sm	1.0	1.05	1.0	1.02
fm3/sm	1.0	1.01	1.00	1.01
ft0/sm	19.10	4.23	3.38	2.90
ft1/sm	15.88	2.23	2.83	2.90
ft2/sm	4.61	1.33	1.35	1.54
ft8/sm	1.0	1.0	1.0	1.31
ft9/sm	1.0	1.0	1.0	1.08

Table 5: Dimension 8 operators and their comparison to SM values. This is for a coupling strength of 10^{-4} TeV.

The WWW was chosen for further study. The main background for the WWW anomalous coupling is SM WWW, followed by dibosons (WW, WZ, ZZ), z+jets, z+photon, w+2jets and ttbar dilepton. With the except of the ttbar background, the other backgrounds are eliminated by using lepton charge and number of leptons cuts. The ttbar background is handled by making a cut on the log of the invariant mass of the 3 leptons to be less than 3.1.

To make this a more realistic study, pile up was added according to the Snowmass scheme [**?**]. The significance was calculated using a LLR calculation and Frequentist approach [**?**]. As can be seen in Figures reffig:t0www14 and 14.

We found that some of the events in the analysis violate unitarity. After taking this into account our significances have change. Figure 15 shows how the significance in a variety of scenarios changes when unitarity bounds are applied.

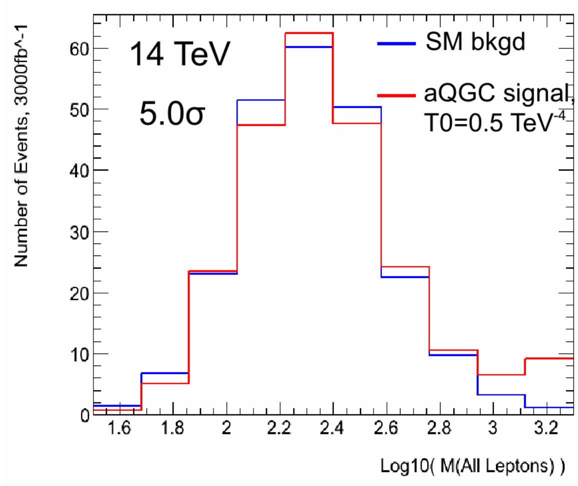

Figure 13: WWW invariant mass with pileup added and backgrounds reduced. The SM is in blue and the mass with $T0$ turned on is in blue.

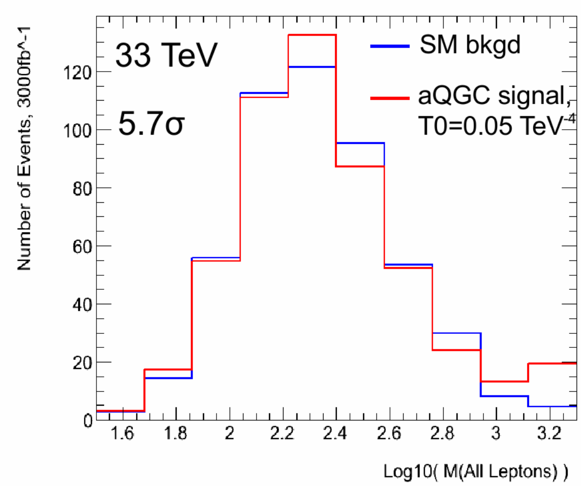

Figure 14: WWW invariant mass with pileup added and backgrounds reduced. The SM is in blue and the mass with $T0$ turned on is in blue.

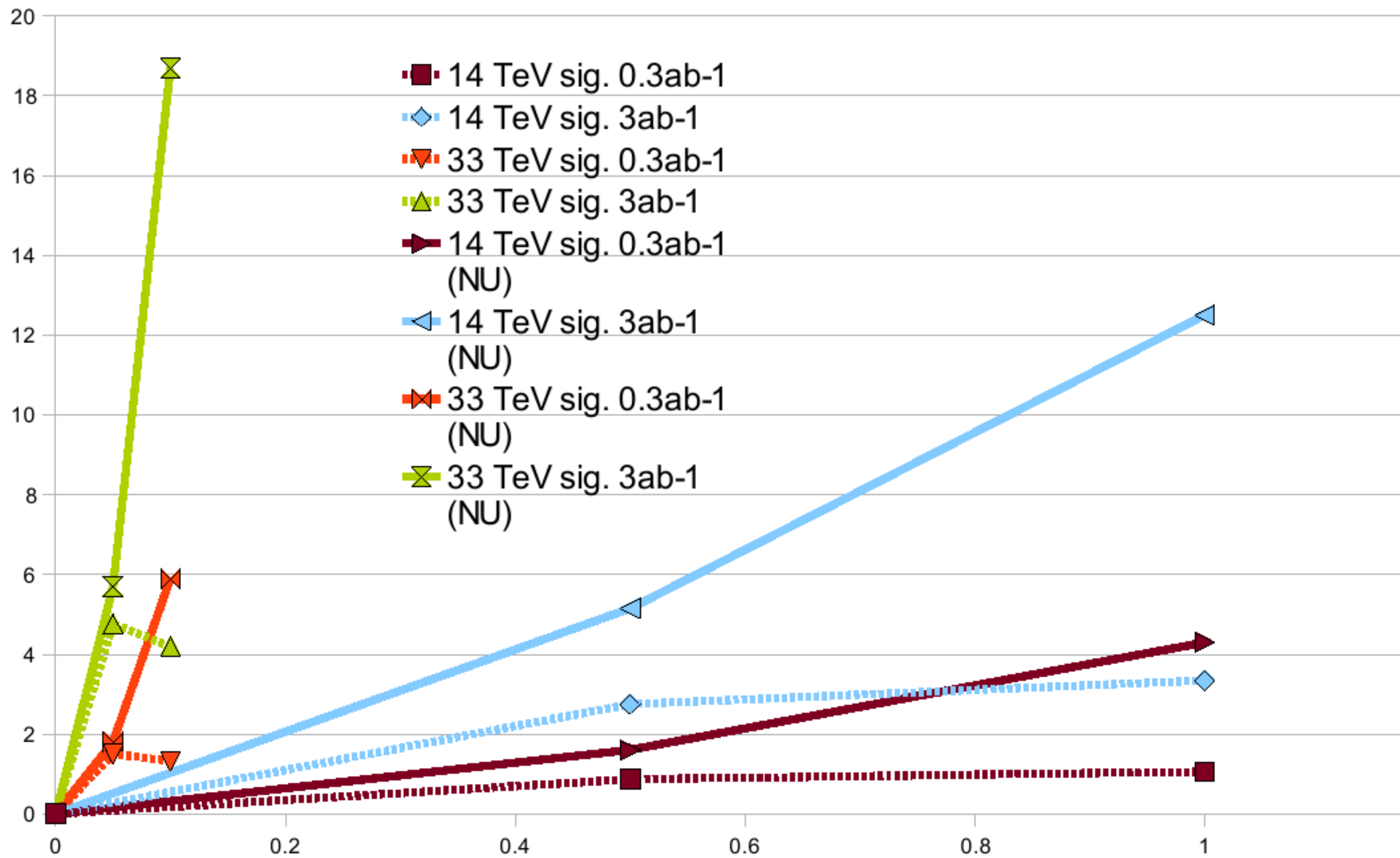

Figure 15: Significance values before unitarity (solid) and after unitarity cuts (dashed) for the $T0$ operator in various scenarios.

5.1 Other Studies

Besides LHC scenarios, the lepton collider scenarios were studied. Future versions of this document will include the ILC scenario table.

6 $Z\gamma\gamma$ in the dilepton plus diphoton channel

The $Z\gamma\gamma$ mass spectrum at high mass is sensitive to BSM triboson contributions. The lepton-photon channel allows full reconstruction of the final state and calculate the $Z\gamma\gamma$ invariant mass. This analysis is new since the European Strategy Submission. We parameterize the BSM physics using the following operators

$$\begin{aligned} \mathcal{L}_{T,8} &= \frac{f_{T8}}{\Lambda^4} B_{\mu\nu} B^{\mu\nu} B_{\alpha\beta} B^{\alpha\beta} \\ \mathcal{L}_{T,9} &= \frac{f_{T9}}{\Lambda^4} B_{\alpha\mu} B^{\mu\beta} B_{\beta\nu} B^{\nu\alpha} \end{aligned} \tag{4}$$

6.1 Monte Carlo Predictions

MadGraph 1.5.10 [2] was used to generate all $Z\gamma\gamma$ samples and background samples, $Z\gamma j$ and Zjj. In both cases Z bosons were required to decay to electron or muon pairs. After Pythia 6 parton showering, the reconstruction effects of resolution and identification efficiency are applied using Delphes [5] with the ATLAS parametrizations. A constant jet-to-photon fake rate of 10^{-3} is applied to each jet in the $Z\gamma j$ and Zjj samples to construct smooth background templates.

6.2 Event Selection

Events are considered $Z\gamma\gamma$ candiates provided they meet the following criteria:

- $p_T(l) > 25$ GeV, $|\eta(l)| < 2.0$
- $p_T(\gamma) > 25$ GeV, $|\eta(\gamma)| < 2.0$
- At least one lepton and one γ with $p_T > 160$ GeV
- $|m_{ll} - 91 \text{ GeV}| < 10$ GeV
- $\Delta(\gamma,\gamma) > 0.4$; $\Delta(l,\gamma) > 0.4$; $\Delta(l,l) > 0.4$.

The 160 GeV transverse momentum requirement on one lepton and one photon improves the sensitivity of aQGC. The 10 GeV invariant mass window cuts around Z boson mass peak can suppresses the $\gamma*$ contribution to the dilepton. The large angle cut between photon and lepton and the high transverse-momentum requirement of the photon reduces the FSR contribution. This leads to the phase space which is uniquely sensitive to the QGC. Figure 16 (left) shows the reconstructed 4-body invariant mass distribution for this channel. Figure 16 (right) shows the enhancement of the yield in the tail of the photon p_T distribution due to anomalous QGC.

6.3 Statistical Analysis

The distribution of $m_{Z\gamma\gamma}$ is used for hypotheses testing by comparing the sum of the SM and background processes to the BSM templates (including backgrounds) obtained from the dimension-8 operators in Eqn. 4. The dominant process in the QGC-sensitive kinematic phase space is the true $Z\gamma\gamma$ production while the fake background $Z\gamma j$ and Zjj are subdominant.

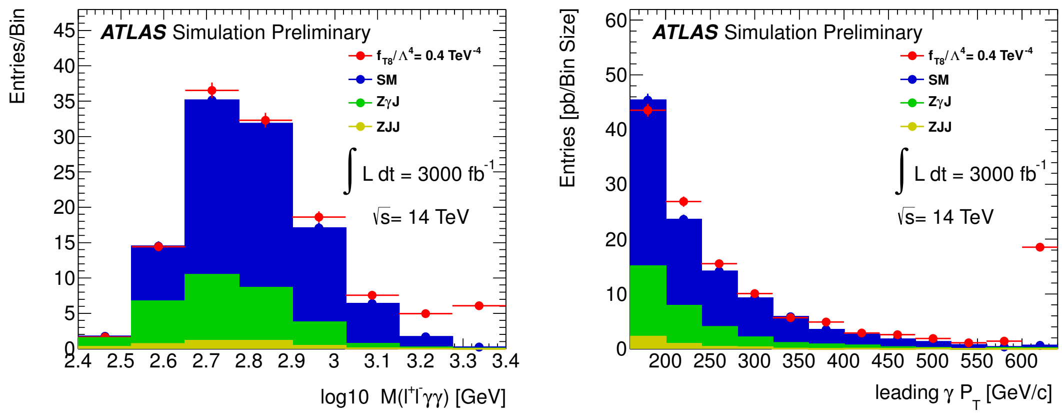

Figure 16: Reconstructed mass spectrum using the charged leptons and photons (left) and leading photon p_T (right) after event selection. The overflow bin is included in each plot.

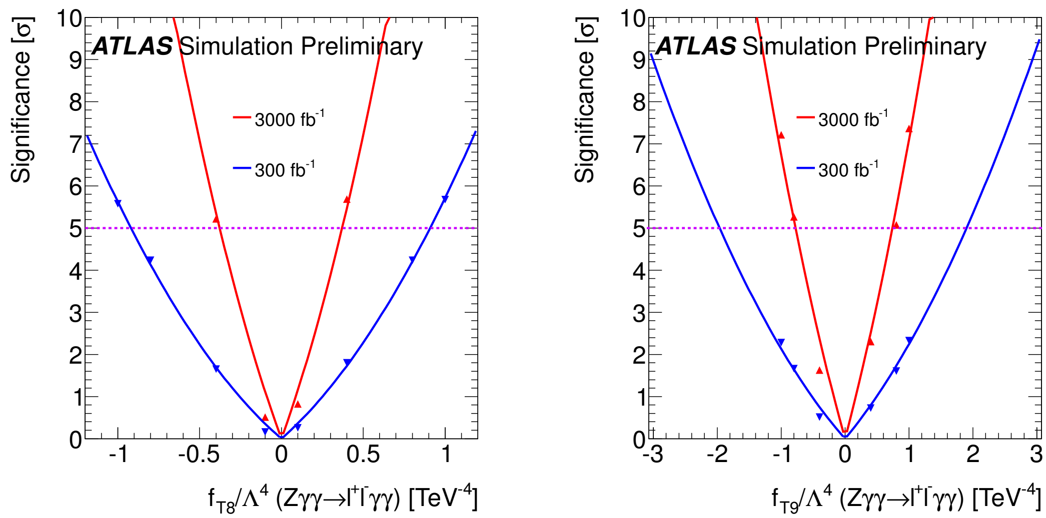

Figure 17: The signal significance as a function of f_{T8}/Λ^4 (left) and f_{T9}/Λ^4 (right).

The statistical analysis is identical to that employed in Sec. 3.3. Figure 17 shows the expected signal significance as a function of BSM physics parameters. Quoted in Table 6 are the 5σ-significance discovery values of the coefficients for an integrated luminosity of $300\,\text{fb}^{-1}$ and $3000\,\text{fb}^{-1}$ respectively.

	$300\,\text{fb}^{-1}$	$3000\,\text{fb}^{-1}$
f_{T8}/Λ^4	$0.9\ \text{TeV}^{-4}$	$0.4\ \text{TeV}^{-4}$
f_{T9}/Λ^4	$2.0\ \text{TeV}^{-4}$	$0.7\ \text{TeV}^{-4}$

Table 6: Summary of expected sensitivity to anomalous $Z\gamma\gamma$ production at $\sqrt{s} = 14$ TeV, quoted in the terms of 5σ-significance discovery values of f_{T8}/Λ^4 and f_{T9}/Λ^4.

References

[1] ATLAS Collaboration, *A Measurement of WZ production in proton-proton collisions at $\sqrt{s} = 8$ TeV with the ATLAS detector*, Tech. Rep. ATLAS-CONF-2013-021, CERN, Geneva, March, 2013. http://cds.cern.ch/record/1525557.

[2] J. Alwall, M. Herquet, F. Maltoni, O. Mattelaer, and T. Stelzer, *MadGraph 5 : Going Beyond*, JHEP **1106** (2011) 128, `arXiv:1106.0522 [hep-ph]`.

[3] ATLAS Collaboration, *Physics at a High-Luminosity LHC with ATLAS*, Tech. Rep. ATL-PHYS-PUB-2012-001, CERN, Geneva, Aug, 2012. http://cds.cern.ch/record/1472518.

[4] ATLAS Collaboration, *Measurement of the total ZZ production cross section in proton-proton collisions at $\sqrt{s} = 8$ TeV in 20 fb^{-1} with the ATLAS detector*, Tech. Rep. ATLAS-CONF-2013-020, CERN, Geneva, March, 2013. http://cds.cern.ch/record/1525555.

[5] S. Ovyn, X. Rouby, and V. Lemaitre, *DELPHES, a framework for fast simulation of a generic collider experiment*, `arXiv:0903.2225 [hep-ph]`.